The Plant Cell, Vol. 20: 3038–3049, November 2008, www.plantcell.org

Maternal Control of Male-Gamete Delivery in *Arabidopsis* Involves a Putative GPI-Anchored Protein Encoded by the *LORELEI* Gene [W]

Arnaud Capron,[a,1] Mathieu Gourgues,[b,2] Lissiene S. Neiva,[b,3] Jean-Emmanuel Faure,[b,4] Frederic Berger,[b,5] Gabriela Pagnussat,[a] Anjali Krishnan,[a] Cesar Alvarez-Mejia,[c] Jean-Philippe Vielle-Calzada,[c] Yuh-Ru Lee,[a] Bo Liu,[a] and Venkatesan Sundaresan[a,6]

[a] Department of Plant Biology, University of California, Davis, California 95616

[b] Ecole Normale Supérieure de Lyon, Unité Mixte de Recherche 5667, Reproduction et Développement des Plantes, Lyon cedex 07, France

[c] National Laboratory of Genomics for Biodiversity, Cinvestav, Guanajuato, Mexico

In Angiosperms, the male gametes are delivered to the female gametes through the maternal reproductive tissue by the pollen tube. Upon arrival, the pollen tube releases the two sperm cells, permitting double fertilization to take place. Although the critical role of the female gametophyte in pollen tube reception has been demonstrated, the underlying mechanisms remain poorly understood. Here, we describe *lorelei*, an *Arabidopsis thaliana* mutant impaired in sperm cell release, reminiscent of the *feronia*/*sirène* mutant. Pollen tubes reaching *lorelei* embryo sacs frequently do not rupture but continue to grow in the embryo sac. Furthermore, *lorelei* embryo sacs continue to attract additional pollen tubes after arrival of the initial pollen tube. The *LORELEI* gene is expressed in the synergid cells prior to fertilization and encodes a small plant-specific putative glucosylphosphatidylinositol-anchored protein (GAP). These results provide support for the concept of signaling mechanisms at the synergid cell membrane by which the female gametophyte recognizes the arrival of a compatible pollen tube and promotes sperm release. Although GAPs have previously been shown to play critical roles in initiation of fertilization in mammals, flowering plants appear to have independently evolved reproductive mechanisms that use the unique features of these proteins within a similar biological context.

INTRODUCTION

In plants, the gametes are not directly generated as products of meiosis, but result from division and differentiation of the multicellular haploid gametophytes. In angiosperms, the gametophytes are the pollen and the embryo sac, producing the male and female gametes, respectively. Furthermore, the male gametes are nonmobile and are instead carried, after germination of the pollen grain on the female stigma, by the pollen tube. The pollen tube emanates from the pollen grain and finds its way in the female tissues, ultimately delivering two sperm cells to the embryo sac, at the mycropylar end. The canonical mature embryo sac, as in *Arabidopsis thaliana*, is composed of seven cells: the egg cell and the central cell, which will receive the two sperm cells, two synergids at the micropylar end, and three antipodal cells at the chalazal end. The proper delivery of the male gametes relies on a series of signals from the embryo sac. Through laser ablation experiments in *Torenia fournieri*, Higashiyama et al. (2001) showed that the synergid is the direct source of attractant for the pollen tube, while recent work in maize (*Zea mays*) has shown that the egg cell may also play a role in this guidance (Dresselhaus, 2006). Furthermore, work by Chen et al. (2007) has shown an involvement of the central cell in the guidance of the pollen tube in *Arabidopsis*. Upon arrival at the embryo sac, the pollen tube releases the sperm cells for the double fertilization to proceed. Furthermore, the embryo sac loses its ability to attract pollen tubes after fertilization is initiated.

Recently, the identification in *Arabidopsis* of the receptor-like kinase FERONIA has shed some light on potential signaling mechanisms responsible for these processes. In *feronia* and *sirène* mutants, the pollen tube can reach the embryo sac, but instead of arresting and delivering the two sperm cells, the pollen tube does not arrest and continues to grow and invades the

[1] Current address: Department of Cell Systems Biology, University of Toronto, 25 Willcocks St., Toronto, ON M5S 3B2, Canada.

[2] Current address: Unité Mixte de Recherche, Interactions Plante Microorganisme et Santé Végétale, Centre National de la Recherche Scientifique/Institut National de la Recherche Agronomique/Unice, 400 Route des Chappes, Sophia Antipolis, F-06903 France.

[3] Current address: Department of Molecular Neurogenetics, McGill University/Montréal Neurological Institute, 3801 Rue University, Montreal, Quebec H3A 2B4, Canada.

[4] Current address: European Commission, Research Directorate General, Research Infrastructures (Unit B3) Office SDME 1/133, B-1049 Brussels, Belgium.

[5] Current address: Temasek Life Sciences Laboratory, 1 Research link, National University of Singapore, Singapore 117604.

[6] Address correspondence to sundar@ucdavis.edu.

The author responsible for distribution of materials integral to the findings presented in this article in accordance with the policy described in the Instructions for Authors (www.plantcell.org) is: Venkatesan Sundaresan (sundar@ucdavis.edu).

[W] Online version contains Web-only data.

www.plantcell.org/cgi/doi/10.1105/tpc.108.061713

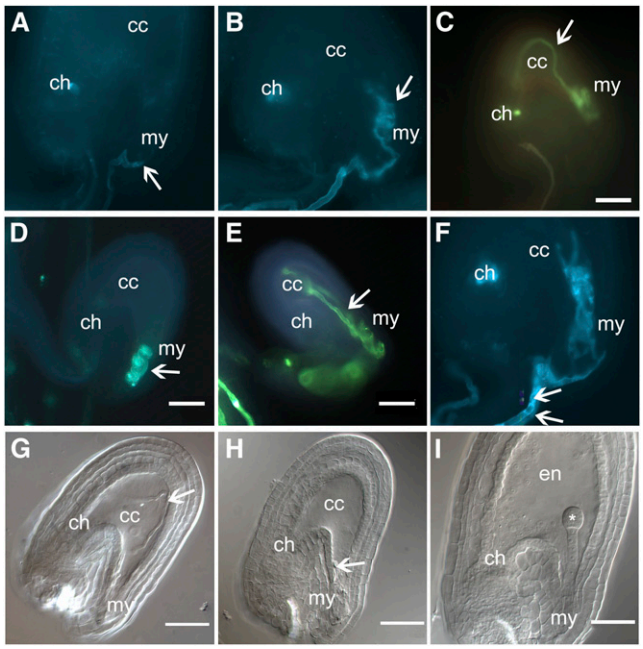

Figure 1. Phenotype of *lorelei* Mutants.

(A) to **(F)** Aniline blue staining of ovules from different *lorelei* mutants pollinated with wild-type pollen.

(A) Wild-type arrival of the pollen tube (arrow) to the micropyle (my). There is no fluorescence inside the ovule.

(B) Pollen tube curling at the micropyle of an *lre-1* ovule.

(C) Pollen tube invading the central cell (cc) and turning back toward the micropyle of an *lre-2* ovule.

(D) Pollen tube curling inside the micropylar end of an *lre-3* mutant.

(E) Pollen tube entering the central cell of an *lre-4* ovule and heading back toward the micropyle.

(F) An example of two pollen tubes reaching the same *lre-1* ovule. The two pollen tubes crawl along the funiculus and enter the embryo sac before forming coils at the micropylar end.

(G) to **(I)** DIC pictures of ovules the same *lre-2*/+ silique pollinated with wild-type pollen.

(G) An example of pollen tube entering deep inside the central cell and turning back toward the micropyle.

(H) Pollen tube coiling at the micropylar end of the embryo sac.

(I) Wild-type-looking ovule with a developed endosperm (en) and an embryo at the dermatogen stage (asterisk).

Arrow, pollen tube; cc, central cell; my, micropylar end; ch, chalazial end; en, endosperm; *, embryo. Bars = 50 μm.

embryo sac (Huck et al., 2003; Rotman et al., 2003). In addition, *feronia*/*sirène* embryo sacs can attract supernumerary pollen tubes (Escobar-Restrepo et al., 2007). *FERONIA* encodes a receptor-like kinase and is expressed in the filliform apparatus, on the surface of the synergid cells (Escobar-Restrepo et al., 2007). *FERONIA* may thus be part of a signaling cascade from the embryo sac to the pollen tube causing growth arrests and allowing sperm cells release. In this model, the ligand of FERONIA can be produced by the pollen. Alternatively, the ligand could be produced the embryo sac itself and FERONIA would be involved in the maturation of functional synergids able to interact with the pollen tube. The *abstinence by mutual consent* (*amc*) *Arabidopsis* mutant (Boisson-Dernier et al., 2008) displays an absence of release of the sperm cells from the pollen tube similar to what was observed in *feronia*/*sirène*. However, this mutant differs from *feronia* in that the defect appears only when a pollen tube from an *amc* pollen grain encounters an *amc* embryo sac, and mutant embryo sacs are fully competent to receive wild-type pollen. The *AMC* gene encodes a peroxin expressed in a wide range of vegetative tissues and strongly expressed throughout both male and female gametophytes. AMC appears to be necessary for PTS-1–dependent peroxisome import and may be involved in the processing of a ligand or some other signaling steps in the recognition pathway for both the pollen and the embryo sac. In this study, we describe an *Arabidopsis* mutant, *lorelei*, whose phenotype is reminiscent of the *feronia*/*sirène* mutation. *lorelei* embryo sacs show an impairment of fertilization caused by an inability of the pollen tube to release the sperm cells upon arrival at the *lorelei* embryo sac. The pollen tube subsequently experiences a continuous growth, resulting in an invasion of the embryo sac. The *LORELEI* gene encodes a putative plant-conserved glucosylphosphatidylinositol (GPI)-anchored protein (GAP) and is expressed in the synergid cells of the embryo sac. We thus identify a second female gametophyte-specific component of the signaling pathway or pathways required for fertilization in higher plants.

RESULTS

The *lorelei* Mutation Causes an Invasive Pollen Tube Phenotype and Failure of Fertilization

To obtain more data on the role of the embryo sac in pollen tube guidance, we performed a genetic screen to isolate mutants deficient in pollen tube reception and pollen tube arrest typical of the *sirène* class represented by the two alleles *srn* and *fer*. Plants from a population of Columbia (Col) wild-type seeds irradiated by gamma rays were used as pollen donors to fertilize wild-type ovules. We did not obtain male gametophytic mutants defective for fertilization among 2000 lines. However, we isolated mutant lines that showed >25% of seeds arrested at early stages after self-fertilization. The line GM474 showed a phenotype similar to *srn* and *fer*. Ovules from self-fertilized *lre-1*/+ plants showed

Table 1. Transmission of *lre* for the *lre-1* and *lre-2* Deletions

Ovule × Pollen	*lre*/+	Wild Type	Ratio *lre-1*/Wild Type
lre-1/+ × Col	19	224	0.08:1
Col × *lre-1*/+	142	181	0.78:1
	Kan^r	Kan^s	Ratio Kan^r/Kan^s
lre-2/+ self	983	902	1.09:1
lre-2/+ × *Ler*	43	361	0.12:1
Ler × *lre-2*/+	224	266	0.84:1

The genetic transmission of the *lre* mutation (ovule donor listed first) of the *lre-1* and *lre-2* deletions was established by observation of *lorelei* phenotype (invasive pollen tube) occurrence for *lre-1* and by assaying the transmission of the linked *nptII* gene in *lre-2*.

Table 2. Phenotypic Analysis of *lre-1* and *lre-2* by DIC Analysis

Ovule × Pollen	Col × Col	*lre-1*/+ × *lre-1*/+	*lre-1*/+ × Col	Col × *lre-1*/+	*lre-2*/+ × *lre-2*/+	*lre-2*/+ × L*er*
Normal	257 (95.5%)	140 (50.9%)	149 (58.5%)	202 (95.7%)	431 (55.8%)	138 (65.7%)
Invasive pollen tube	0 (0%)	82 (29.8%)	70 (27.4%)	0 (0%)	221 (28.6%)	54 (25.7%)
Unfertilized	2 (0.8%)	39 (14.2)	31 (12.1%)	6 (2.8%)	95 (12.3%)	3 (1.4%)
Aborted	10 (3.8%)	14 (5.1%)	5 (2.0%)	3 (1.5%)	26 (3.4%)	15 (7.1%)

The flowers were emasculated and fertilized manually with pollen. The phenotype was scored 48 h after pollination using DIC on cleared ovules.

failure of pollen tube arrest with further curling or invasive growth of the pollen tube in the embryo sac (Figure 1B). We tentatively named the mutation carried by GM474 *lorelei-1* (*lre-1*) in reference to the mermaid names used for this class of phenotype. Genetic mapping based on 2108 plants determined that the mutation *lre-1* location is within an interval between the BACs F14M19 and F10M23.

In parallel, we previously described a *Ds* element insertion collection in *Arabidopsis* for gametophytic mutants (Pagnussat et al., 2005). One of these mutants, called *une17* (for *unfertilized embryo sac 17*), displayed a segregation ratio of the kanamycin resistance, carried by the *Ds* element, of 1.09:1, clearly indicative of a gametophytic defect. Furthermore, it proved impossible to recover a plant homozygous for the *Ds* element. Reciprocal crosses with the wild type as an ovule or pollen donor showed a mainly female lethality (0.12:1 and 0.84:1, respectively) and reduced genetic transmission from the female but not from the male gametes (Table 1). Differential interference contrast (DIC) observation of cleared heterozygous siliques after pollination showed that 28.6% of the embryo sacs displayed a failure of pollen tube arrest and sperm discharge. Instead, these embryo sacs contained an invasive pollen tube, either curling at the micropylar end (Figure 1H) or entering in the central cell region and then turning back toward the micropyle (Figure 1G). Because of its similarity to the previously identified *lorelei* mutation, which mapped to the same chromosomal region (see below), this mutant was renamed *lorelei-2* (*lre-2*).

Crosses between ovules from *lre*/+ plants and wild-type pollen produced siliques in which approximately one-quarter of the embryo sacs were aborted and had invasive pollen tube growth (Table 2). By contrast, there was very limited ovule abortion in crosses between wild-type ovules and pollen from *lre*/+ plants. The proportion of aborted ovules with invasive pollen tube growth between *lre*/+ siliques pollinated with wild-type pollen and self-pollinated *lre*/+ siliques showed little variation. However, ~10% of the seeds aborted in self-pollinated *lre*/+ plants as a result of early embryo and endosperm arrest between the 2- to 8-cell stage in the embryo. Although the *Ds* element insertion primarily affected the embryo sac function, there was also some reduced transmission of the transposon through the *lre-2* pollen, but we did not detect a reduced transmission through *lre-1* pollen (Table 1), indicating that the pollen defect might be allele specific. In conclusion, the mutations *lre-1* and *lre-2* primarily affect the capacity of the embryo sac to be fertilized, and the phenotype exhibits a moderate penetrance.

To confirm the observations made with DIC on cleared ovules, the phenotypes were rescored using samples stained with aniline blue. This method allow for easy visualization of the pollen tube (Figures 1A to 1C, Table 3). In both *lre* deletions, the proportion of embryo sacs showing an invasion by a pollen tube was similar to the one observed with DIC. We were also able to score the number of pollen tubes reaching a single ovule using aniline blue staining. Table 4 shows that embryo sacs in *lre*-/+ can attract supernumerary pollen tubes, as >20% of the ovules had two or more pollen tubes reaching them (Figure 1F). Overall, the defects observed in *lre*/+ siliques are quite similar to those described in the *feronia*/*sirène* (Huck et al., 2003; Rotman et al., 2003) and *amc* mutants (Boisson-Dernier et al., 2008), with an overgrowth of the pollen tube in the embryo sac and attraction of supernumerary pollen tubes. However, the penetrance of the *lre-1* and *lre-2* mutations is lower than what was observed in *feronia*/*sirène*. While ovules from *fer*/+ siliques showed invasion by the pollen tube almost 50% of the time, the percentage of occurrence in *lre-2* is lower at 25%. These observations, in addition to the possible transmission of *lre* through the female suggest that the defect is not as drastic in *lre-2* compared with *fer* and *srn*, which are not transmitted through the female gametes (Huck et al., 2003; Rotman et al., 2003). A direct comparison with *amc* is not possible because while *lre-2* and *fer* are independent of the male gametophyte, the *amc* phenotype appears only if both the pollen and the embryo sac carry the mutation, and *amc* embryo sacs are able to receive wild-type pollen normally (Boisson-Dernier et al., 2008).

To examine whether the invasive pollen tube phenotype observed in *lre*/+ siliques arose from defective embryo sac development, analysis using DIC of the developing embryo sacs was performed. No defects could be observed during embryo sac development, and the mature, unpollinated embryo sacs appeared uniformly normal in *lre*/+ siliques. Furthermore, ovules from *lre-1*/+ plants expressed the β-glucuronidase reporters for the genes *MEA* and *FIS2* the same those from the wild type. Similarly, *lre-2*/+ correctly expressed the β-glucuronidase genes associated with the embryo sac marker lines ET119 and ET2634 (Gross-Hardt et al., 2007) in specific cell types in the embryo sac, the egg cell, and the synergids (data not shown). Similar experiments performed on *feronia* also failed to show defects during the embryo sac development (Huck et al., 2003).

Table 3. Phenotypic Analysis of *lre-1* and *lre-2* by Aniline Blue Staining

	lre-1/+ × Col Pollen	*lre-2*/+ × L*er* Pollen
Normal	305 (78.8%)	338 (67.6%)
Invasive pollen tube	82 (21.2%)	136 (27.2%)
No fluorescence	0 (0%)	26 (5.2%)

The phenotype scoring was repeated using aniline blue staining 48 h after pollination on *lre* siliques pollinated with wild-type pollen.

Table 4. Polyspermy in *lre* Mutants

	Col × Col	*lre-1*/+ × Col pollen	*lre-2*/+ × L*er* Pollen
One pollen tube	493	239	193
Two pollen tubes	8 (1.6%)	49 (20.5%)	48 (19.8)
Three pollen tubes	0 (0%)	2 (0.1%)	1 (0.4%)

Supernumerary pollen tubes reaching the embryo sac were counted using aniline blue staining 48 h after pollination.

Molecular Characterization of *lre-1* and *lre-2*

The *lre-1* mutation was caused by gamma ray irradiation, and we could not obtain new recombinants after scoring 1200 plants in our collection of 2100 F2 mapping population. We made the hypothesis that a deletion took place at the *lre-1* locus. To determine the extent of the potential deletion, we made crosses between wild type Landsberg *erecta* (L*er*) and *lre-1*/+ in the Col background to produce F1 hybrids carrying the mutation. We tried to detect polymorphism between Col and L*er* across the genetic location previously determined by mapping. Polymorphism was not detected in *lre-1*/+ Col-0/L*er* hybrids inside a region delimited by the genes *At4g26190* and *At4g26570*, comprising at least 63 open reading frames (ORFs). The lack of polymorphism indicates the deletion causing the *lre* phenotype must encompass this region spanning 160 kb on the chromosome 4 (Figure 2A). In the case of *lre-2*, the *Ds* element mutagenesis allows for recovery of the sequences flanking the insertion site by thermal asymmetric interlaced (TAIL)-PCR (Liu et al., 2005). Initial experiments placed the 5′ end of the *Ds* element of *une17/lre-2* in the second exon of the gene *At4g26330* (Pagnussat et al., 2005). Further TAIL-PCR analysis indicated that the 3′ end of the transposon is inserted in 5th exon

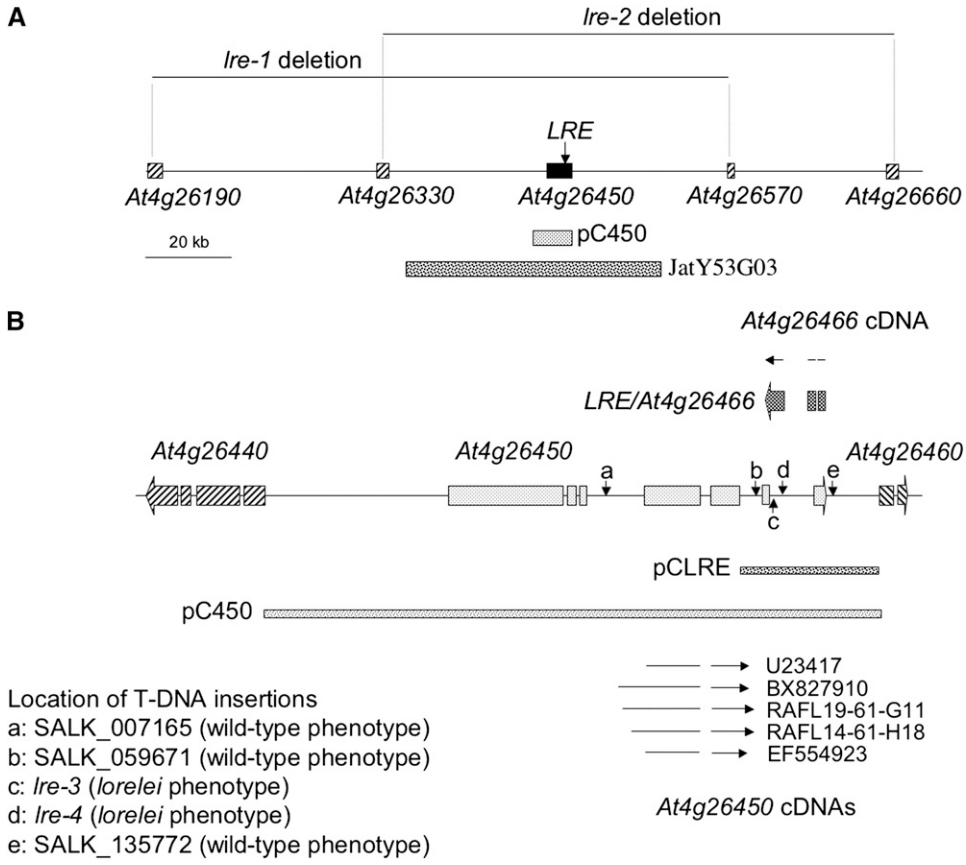

Figure 2. Structure of the *LORELEI* Locus and Its Vicinity.

(A) A schematic view of the region of chromosome 4 showing the position of *At4g26450* and *At4g26466* as well as the extent of the deletions present in *lre-1* ad *lre-2*. The sequences covered by the complementation constructs JatY53G03 and pC450 are displayed as well.

(B) Close-up drawing of the *At4g26450*/*At4g26466* locus. The map shows the structure of *At4g26450* (seven exons, light gray boxes on the map) and *At4g26466* (three exons, dark-gray boxes above the map) as annotated by the Arabidopsis Genome Initiative consortium as well as the two bordering genes, *At4g26440* and *At4g26460*. The full-length cDNAs for *At4g26450* present in the database are shown (as arrows indicating the exons, below the schematic) as well at the cDNA for *At4g26466* (arrow above the schematic) produced during this work. Furthermore, the positions of the five T-DNA lines investigated are also marked by the vertical arrows. The two T-DNA lines with an *lre* phenotype (*lre-3* and *lre-4*) are marked as c and d. The three other lines had a wild-type phenotype. Finally, the length of complementing constructs pC450 and pCLRE is also displayed.

Table 5. Complementation of *lre-2*

	Kan^r	Kan^s	Ratio Kan^r/Kan^s
lre-2/+; JatY53G03-1	185 (68.5%)	85 (31.5%)	2.18:1
lre-2/+; JatY53G03-5	231 (74.3%)	80 (25.7%)	2.89:1

lre-2/+ plants were transformed with the JatY53G03 binary vector, and the segregation of the linked *nptII* gene conferring kanamycin resistance (Kan^r) was scored in the T2 generation. Kan^s, kanamycin sensitivity.

of *At4g26660*, at a distance of 128.2 kb from the 5′ flanking sequence. PCR using gene-specific primers confirmed the results of the TAIL-PCR on *lre-2*/+ genomic DNA. Therefore, the insertion of the *Ds* element seems to have caused the deletion of a 128-kb stretch of chromosome IV, affecting 41 annotated genes or pseudogenes (Figure 2A).

To confirm that the phenotype observed in *lre-2*/+ siliques was indeed caused by this deletion, we transformed *lre-2*/+ plants with a binary vector, JatY53G03, containing a section of the chromosome IV, including the genes from *At4g26350* to *At4g26530* (Figure 2A). The resulting T2 plants were screened for complementation of the *Ds* transmission frequency using the Kan^r/Kan^s ratio. Several independent transformants displaying an increase in Kan^r/Kan^s were recovered (Table 5). The line *lre*-2/+;JatY53G03-1/+ was further characterized for pollen tube invasion in the embryo sac as well as the Bar^r/Bar^s ratio, indicative of the complementing construct that confers resistance to Basta. As shown in Tables 6 and 7, the invasive pollen tube phenotype was entirely rescued in the progeny of the T2 plants 1.2 of the complementing line, corresponding to the complementing construct in a homozygous state, as indicated by the complete Basta resistance in this family.

This complementation experiment indicated that the locus responsible for the *lorelei* phenotype was located between *At4g26350* and *At4g26530*. To identify the specific gene, all of the 19 annotated genes present on JatY53G03 were independently cloned in binary vectors and transformed in *lre-2*/+ plants. The F2 progeny from those transformants were screened for their Kan^r/Kan^s ratio. However, we noted that one of the genes contained in the original deletion, and also on the complementing BAC JatY53G03, was *At4g26500*, which has been identified as embryo lethal (Xu and Møller, 2006). Therefore, the expected ratio after rescue in the case of a single copy of the complementing construct containing a single gene would be 2:1 at best. Of the 17 constructs tested, only one construct, pC450 (Figure 2A), resulted in a significant increase of Kan^r/Kan^s ratio, as shown in Table 8.

Identification of Additional *lorelei* Alleles

The vector pC450 contained ~10 kb of *Arabidopsis* genomic DNA surrounding *At4g26450*. Several T-DNA insertion lines were available in this region, and five of them were investigated further (Figure 2B). Three of those lines did not display any invasive pollen tube phenotype (SALK_007165, SALK_059671, and SALK_135772). However, the lines SALK_040289 and SAIL_8_C08 presented the same invasion of the embryo sac by the pollen tube as the *lre* mutants (Figures 1D and 1E) and were renamed *lre-3* and *lre-4*, respectively. Observations made on siliques from *lre-3*/+ and *lre-4*/+ showed a similar penetrance of the invasive pollen tube phenotype in those lines (Table 9). A homozygous line for *lre-3* was recovered and analyzed. The occurrence of the *lorelei* phenotype in the homozygote was double what was observed in the *lre-3* heterozygote, as expected from twice the number of mutant embryo sacs in the homozygote (Table 9). Importantly, the homozygous knockout plants were healthy and had no other visible phenotypes, suggesting that the *LRE* gene functions specifically in fertilization. While the *lre-3* homozygous line displayed a strong increase in invasive pollen tube frequency, half of the mutant embryo sacs are able to receive the pollen tube normally. It could therefore be hypothesized that the function of *LRE* in the signaling pathway is partially redundant and/or is, to some extent, dispensable (see below).

Isolation of the *LORELEI* Gene

When the work to identify the *LORELEI* gene was performed, the gene *At4g26466* was not annotated. In silico analysis of the region lead to the discovery of another gene at the *At4g26450* locus, which was identified as *LORELEI* and appears under the number *At4g26466* in the AGI V8 annotation (see Supplemental Results online). To confirm that *At4g26466* was indeed *LORELEI*, a construct covering the sequences between the exon 5 of *At4g26450* and the stop codon of *At4g26460* was transformed in *lre-3* homozygotes and able to rescue the phenotype (Table 10). Furthermore, a cDNA matching the sequence of the predicted *At4g26466* was recovered through RT-PCR (see Supplemental Results online).

LORELEI Is Expressed in the Synergid Cells of the Embryo Sac

Preliminary studies showed that *LORELEI* was expressed at a low level throughout the plants, including in floral organs (see Supplemental Results online). To determine the pattern of localization of *LORELEI* mRNA, we performed in situ hybridization in

Table 6. Rescue of the Invasive Pollen Tube Phenotype by JatY53G03

	lre-2/+; JatY53G03-1.2	*lre-2*/+; JatY53G03-1.4	*lre-2*/+; JatY53G03-1.6
Normal	164 (92.1%)	151 (77.3%)	168 (77.1%)
Invasive pollen tube	0 (0%)	36 (18.6%)	32 (14.7%)
No pollen tube	8 (4.5%)	4 (2.1%)	10 (4.6%)
Aborted	6 (3.4%)	3 (1.5%)	8 (3.7%)

Plants carrying the *lre-2* mutation and the JatY53G03 construct were tested for invasive pollen tubes 48 h after pollination using DIC.

Table 7. Segregation of the Kan^r and Bar^s Markers in the *lre-2*/+ Transformed Lines

	Kan^r	Kan^s	Bar^r	Bar^s
lre-2/+; JatY53G03-1.2	366 (71.9%)	143 (28.1%)	100%	/
lre-2/+; JatY53G03-1.4	157 (66.8%)	78 (32.2%)	355 (79.1%)	89 (20.1%)
lre-2/+; JatY53G03-1.6	156 (63.9%)	88 (36.1%)	426 (75.4%)	112 (20.8%)

Segregation ratio for kanamycin and Basta resistance (Kan^r and Bar^s, respectively) in the rescued lines.

longitudinal sections of wild-type ovules, using a digoxygenin-labeled probe of 181 bp corresponding to a small portion of the 3rd exon in *At4g26466*. We find that *LORELEI* expression occurs in differentiated ovules that contain cellularized female gametophytes prior to pollination. Specifically, *LORELEI* mRNA was localized in the egg apparatus, predominantly in both synergids prior to degeneration (Figure 3A). Sporadically, a weak signal was detected in the cytoplasm of the egg cell (Figure 3A); however, no mRNA was localized in the central cell and the antipodals either before or after pollination. After pollination, abundant mRNA was found localized in synergids at the micropylar pole of the female gametophyte (Figures 3B and 3C). Although this signal could reflect a higher concentration of mRNA confined to a restricted portion of cytoplasm in degenerating synergids, it could also be the result of an increase in *LORELEI* expression following pollination. Developing ovules undergoing megasporogenesis or megagametogenesis did not show *LORELEI* mRNA localization at any developmental stage, indicating that LORELEI is active only in the fully differentiated cells of the egg apparatus.

LORELEI Encodes a Conserved, Plant-Specific, GPI Anchor Protein

Sequence comparison of the predicted protein showed strong similarity with a small family of GAPs with three known members in *Arabidopsis* and more in other plants, including rice (*Oryza sativa*), maize, and *Physcomitrella patens*. Using BLAST (Altschul et al., 1990) with the LORELEI sequence against the *Medicago truncatula* and *Populus trichocarpa* genome allowed the identification of partial sequences of three putative orthologs in *Medicago* and one in *Populus*. Performing the same type of analysis as used for LORELEI (see above and Supplemental Results online), it was possible to reconstruct four full ORFs sharing similar gene structures between themselves and with LORELEI. The newly identified ORFs have been named Mt LORELEI-related 1, 2, 3, and Pt LORELEI-related1 for the *Medicago* and poplar sequences, respectively.

No significant similarities were found with animal or yeast proteins. Further in silico analysis of the LORELEI sequence using SignalP (Nielsen et al., 1997; Bendtsen et al., 2004) and TargetP (Emanuelsson et al., 2000) predicted a signal peptide for the secretory pathway containing the first 20 amino acids. BigPI (Eisenhaber et al., 2003), a program designed to detect GPI modification site in plant proteins, found a putative GPI anchor domain in the C terminus, along with a GPI anchor attachment site, Ser-139 (Figure 4A). The presence of an N-terminal signal peptide and a C-terminal anchor signal leaves a central portion of LRE as the potential active domain.

A ClustalW alignment (Larkin et al., 2007) is shown on Figure 4B, displaying a central conserved domain. The domain does not show any similarity with previously described protein domains and appears specific to the LORELEI protein family. Within the domain, several amino acids are conserved in all sequences, such as a series of Cys residues (C62, C72, C73, C81, C117, and C126) as well as several hydrophobic residues (M98, F99, F113, and L124). However, the significance of those conserved residues is unclear. Outside of the central domain, little conservation is observed, particularly in the N-terminal signal peptide and the C-terminal GPI anchor signal. Out of the three identified *LRE* paralogs, *At5g56170* is the closest, with 58% identity and 76% similarity. The two remaining (*At4g28280* and *At2g20700*) show more differences, with 55 and 46% identity and 71 and 65% similarity, respectively. However, *At4g28280* and *At2g20700* are highly similar to each other, showing 83% identity. Both *At2g20700* and *At4g28280* have been found to be expressed strongly in the mature pollen tube in an earlier study, while *At5g56170* was not detected in the same experiment (Lalanne et al., 2004).

To address the intracellular localization of the LRE protein, a green fluorescent protein (GFP) fusion was engineered between the signal peptide and the rest of LRE. First, a modified GFP protein was created with the N-terminal signal peptide of LRE. This modified GFP was fused to the central domain and the GPI anchor domain of LRE to generate an N-signal peptide-GFP-LRE-C fusion (Figure 5A). Unfortunately, efforts to obtain GFP fluorescence in a transient expression experiment by particle bombardment in intact onion cells were not successful with this fusion, although strong expression was obtained with a 35S-GFP control plasmid (data not shown). This suggested the possibility that the fusion protein might be unstable or that it was quenching the GFP fluorescence. Another possible reason for the failure to detect GFP fluorescence in intact tissues might be that localization of the fusion protein on

Table 8. Complementation of *lre-2*/+ by the pC450 Construct

	Kan^r	Kan^s	Ratio Kan^r/Kan^s
lre-2/+; pC450.6-2	235 (67.0%)	116 (33.0%)	2.02:1
lre-2/+; pC450.6-3	155 (51.8%)	144 (48.2%)	1.08:1
lre-2/+; pC450.7-4	249 (66.6%)	125 (33.4%)	1.99:1
lre/-2+; pC450.7-7	255 (66.4%)	129 (33.6%)	1.98:1

lre-2/+ plants were transformed with the binary vector pC450 carrying the annotated *At4g26450* gene. Complementation was confirmed in several independent transformed lines by checking the segregation of the *nptII* gene conferring kanamycin resistance (Kan^r) linked to the *lre-2* mutation. Kan^s, kanamycin sensitivity.

Table 9. Phenotypic Analysis of *lre-3* and *lre-4* by Aniline Blue Staining

	lre-3/*lre-3* × Col pollen	*lre-4*/+ × Col pollen
Normal	195 (54.0%)	280 (74.3%)
Invasive pollen tube	166 (46.0%)	97 (25.7%)

Phenotypic analysis of *lre-3*/*lre-3* and *lre-4*/+.

the outer leaflet of the plasma membrane, predicted for a GPI anchor protein, results in exposure of GFP to unfavorable conditions in the extracellular environment, such as low pH, as noted by others (Nadeau and Sack, 2002; Zheng et al., 2003). Therefore, an alternate system for expression was attempted, which relied upon transfection into isolated *Arabidopsis* mesophyll protoplasts (Yoo et al., 2007). This system permits use of a buffer-controlled environment for the outer surface of the plasma membrane and also has the advantage that it avoids having to employ a heterologous plant system. Using this expression system, with the 35S promoter driving transcription of the LRE-GFP fusion, GFP fluorescence was observed in 10% of the transfected cells, and was in all cases localized to the surface of the protoplasts (Figures 5D and 5G). No GFP signal was detected in the untransfected samples (Figures 5B and 5E), while a positive control using 35S-GFP resulted in very strong cytoplasmic signal that did not localize to the surface of the protoplasts (Figures 5C and 5F). These results are consistent with the predicted localization of LRE to the plasma membrane, at least in *Arabidopsis* protoplasts.

DISCUSSION

GAPs are eukaryotic proteins known to function in cell–cell signaling, and are anchored at their C termini to the extracellular surface of the plasma membrane of the cell though the GPI moiety (Muñiz and Riezman, 2002). The GPI anchor is synthesized in the endoplasmic reticulum membrane in a multistep process, and the processed protein is ultimately trafficked to the cell surface, where it is believed to be tethered to lipid rafts (Orlean and Menon, 2007). GAPs can be released from their anchor into the extracellular medium; this release can be catalyzed by phospholipase C or by ACE (reviewed in Sharom and Lehto, 2002; Mayor, 2005). Only a few genes encoding GAPs have been characterized in terms of function in *Arabidopsis*. The gene *COBRA* is required for polarized cell expansion in the root (Schindelman et al., 2001), and the gene *NDR-1* is involved in signal transduction during disease resistance (Coppinger et al., 2004). A classical arabinogalactan protein containing a GPI anchor has been shown to be involved in the initiation of female gametogenesis in *Arabidopsis* and has been proposed to be involved in intercellular signaling between sporophytic and gametophytic cells (Acosta-Garcia and Vielle-Calzada, 2004). In addition, three *Arabidopsis* mutants affecting biosynthesis of the GPI anchor have also been described. Mutations in two *Arabidopsis* genes, *SETH1* and *SETH2*, encoding *Arabidopsis* homologs of two subunits of the enzymatic complex responsible for the first step of the GPI synthesis, have been shown to be male sterile, preventing pollen germination and pollen tube growth. The *peanut1* mutant, which is defective for another enzyme of the GPI synthesis pathway, is seedling lethal and causes severe morphological defects in the embryo (Gillmor et al., 2005). However, the lack of GPI synthesis did not affect the fertility of the embryo sac in the above mutants. It is plausible that maternally produced enzymes are carried over during the development of the female gametophyte and can synthesize sufficient GPI for *LRE* function, as illustrated by mutations in many essential biosynthetic genes that result in embryo arrest rather than in gametophytic defects (Tzafrir et al., 2004).

The function of *LRE* appears specific to the process of fertilization because *lre* mutant homozygous plants are otherwise normal with no observable growth or developmental defects, consistent with the observed expression pattern of *LRE* with the highest expression in the synergids within the ovule. In mammals, GAPs appear to be critical for fertilization, as mouse eggs lacking GAPs on their surface, generated by conditional knockout of GPI synthesis, are unable to fuse with the sperm (Alfieri et al., 2003; Primakoff and Myles, 2007). GAPs expressed on the surface of mammalian sperm cells are also important for fertilization because cleavage of these proteins by ACE and release into the extracellular medium are required for sperm cell capacitation in oocyte binding (Kondoh et al., 2005). In mammals, species specificity in fertilization occurs through the interactions between sperm cell and egg cell, with cell surface proteins acting as key determinants (reviewed in Wassarman, 1999; Vieira and Miller, 2006). In flowering plants, barriers are provided by the sporophytic tissues, such as the stigma and transmitting tract, and play a major role in preventing interspecies fertilization for distantly related species. In the case of more closely related plant species, it has been demonstrated that species specificity occurs at the stage of the release of sperm from the pollen tube after penetration of the synergid cell (Escobar-Restrepo et al., 2007). Our study shows that although flowering plants and mammals have evolved very divergent mechanisms for fertilization and species recognition in reproduction, in both cases, GPI anchor proteins are used to regulate key steps in fertilization.

Table 10. Complementation of *lre-3* by pC450 and pCLRE

	lre-3/*lre-3*; pC450	*lre-3*/*lre-3*; pCLRE-1	*lre-3*/*lre-3*; pCLRE-3
Normal embryo sacs	246 (89.13%)	161 (85.63%)	206 (81.74%)
Invasive pollen tube	29 (2.42%)	11 (5.85%)	31 (12.30%)
No pollen tube	4 (1.45%)	31 (12.30%)	15 (5.95%)

lre-3 homozygous plants were transformed by pC450 carrying the annotated *At4g26450* gene or pCLRE, a binary vector carrying the *lorelei* genomic sequence. Complementation was assayed by scoring the *lre* phenotype 48 h after pollination using aniline blue staining.

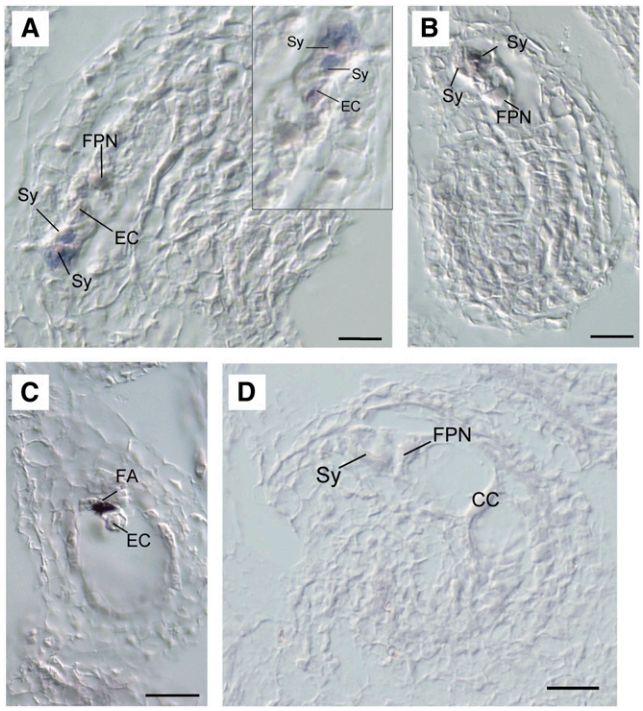

Figure 3. Localization of *LORELEI* mRNA in Wild-Type Ovules of *Arabidopsis*.

(A) Longitudinal section of a fully differentiated ovule prior to pollination, showing predominant *LORELEI* expression (purple color) in both synergids. Inset: a higher magnification of the egg apparatus in a consecutive section of the same ovule shows additional weak expression in the egg cell cytoplasm.

(B) Longitudinal section of a fully differentiated ovule following pollination. *LORELEI* mRNA is localized in both degenerating synergids but not in the central cell.

(C) Longitudinal section of a fully differentiated ovule following pollination. Abundant *LORELEI* mRNA is localized in the remnants of a degenerating synergid.

(D) Longitudinal section of a fully differentiated ovule hybridized with a *LORELEI* sense probe.

Sy, synergid; EC, egg cell; FPN, fused polar nuclei; FA, filiform apparatus; CC, central cell. Bars = 20 μm.

While the specific role of *LRE* in the communication between the pollen tube and the embryo sac remains to be elucidated, the known properties of GAPs suggest some models for future studies. *LRE* might act in the signaling pathway informing the embryo sac of the arrival of a pollen tube, acting in concert with the *FER* receptor kinase, for example, by modifying the lipid microenvironment (van Meer, 2002) to regulate FER localization or function, or downstream in the intracellular response, as exemplified by the GAP protein NDR1 in pathogen defense (Day et al., 2006). The result would be to trigger a signaling cascade in the synergid cell, eventually sending back a signal to the pollen tube, which causes the release of the sperm cells and also shutting down the attraction signal for other pollen tubes. An alternate hypothesis is that *LRE* itself could be part of the arrival signal for the pollen tube, either through its presence on the outer surface of the plasma membrane or through release from the membrane by cleavage of the anchor, perhaps in response to activation of the *FER* kinase. In the former case, the presence of LRE protein would cause an initial response in the pollen tube rather than in the embryo sac. These possible roles of *LRE* could be explored in the future by studies of LRE protein localization in the embryo sac during fertilization and in wild-type and *feronia* mutants and of protein interactions with FER kinase. Because the fusion of LRE to a GFP tag did not exhibit fluorescence in intact plant tissues, protein localization studies await the availability of antibodies to the LRE protein. Another question to be addressed is the potential function of the three *LRE* paralogs. The incomplete penetrance of *LRE* alone could be explained by redundancy with one or more of those genes that are involved in the same pathway. Examination of knockout mutants for *At5g56170*, *At2g20700*, and *At4g28240* have not revealed any mutant phenotypes (G. Pagnussat, unpublished results); therefore, construction of double or triple mutants are needed to shed light on this issue. Finally, studies of *LRE*-related genes in other plant species could yield useful information on the set of the species-specific factors involved in sperm release in flowering plants.

METHODS

Genetic Screen and Mapping

The line GM 474 (Col-0 accession background) was obtained from the genetic screen of γ-ray mutagenized *Arabidopsis thaliana* seeds previously described (Guitton et al., 2004) and was crossed with wild-type L*er* to generate F1 plants heterozygous for polymorphic markers between Col and L*er*. The F1 mutant plants were allowed to self to generate F2 mapping populations. A mapping population of 2108 F2 plants from the GM474 line was analyzed. Markers for mapping were designed using the polymorphisms of the Cereon (www.arabidopsis.org/Cereon/index/html) online database.

Plant Transformation and Selection

Three-week-old *Arabidopsis* plants were transformed by in planta transformation (Bechtold and Pelletier, 1998) with *Agrobacterium tumefaciens* strain GV3101.

Seeds were surface-sterilized and plated onto medium (half-strength Murashige and Skoog salts, 1% sucrose, and 0.9% agar, pH 5.7) supplemented with 50 mg/L kanamycin (for *lre-2*/+), 50 mg/L kanamycin and 6 mg/L gluphosinate (for *lre-2*/+ transformed with JatY53G03), 50 mg/L kanamycin and 15 mg/L hygromycin (for *lre-2*/+ transformed with pC450), or 15 mg/L hygromycin (for *lre-3*/- and *lre-4*/+ transformed with pC450). After 2 d at 4°C, the plates were transferred to a Percival growth chamber (Percival Scientific) with a 16-h-light/8-h-dark cycle at 22°C. Antibiotic resistance was scored after 2 weeks. Plants were then transferred on soil and grown under the condition described above with 60% humidity.

For crosses, flowers of the ovule donor were emasculated and manually pollinated 48 h later.

Cleared Whole-Mount Ovule

For *lorelei* phenotyping analysis, flowers were emasculated and pollinated 48 h later with either wild-type pollen or self pollen. After 2 d, the fertilized pistils were collected and the replum cut open under a dissecting scope. The pistils were then fixed for 1.5 h in an acetic acid/ethanol solution (1:9 [v/v]) and cleared for 24 h in Hoyers solution (Liu and Meinke, 1998). The pistils were then dissected and the ovules observed under a Zeiss Axioplan

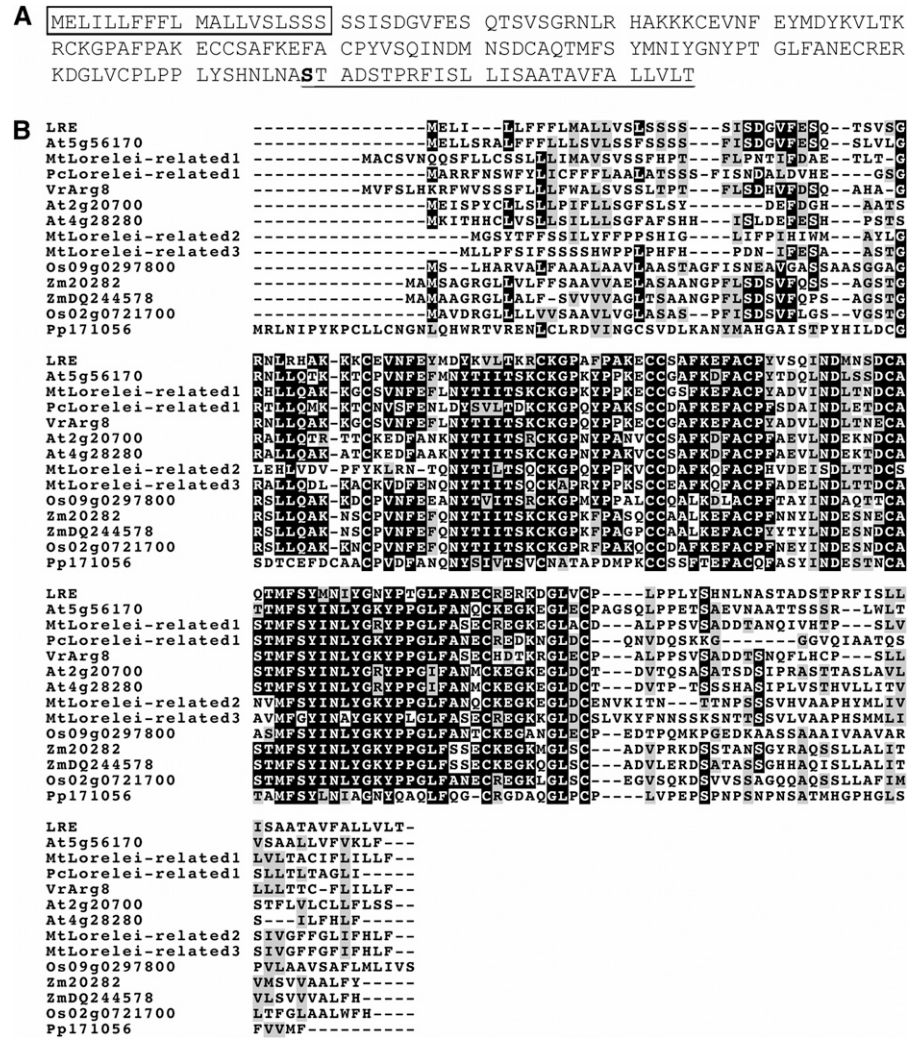

Figure 4. Analysis of the LORELEI Sequence.

(A) Sequence of the LORELEI protein, with the position of the predicted signal peptide (box), the GPI anchor domain (underline), and the Ser binding to the GPI moiety (in bold).

(B) ClustalW alignment of LRE-related proteins from *Arabidopsis* (At), *O. sativa* (Os), *Z. mays* (Zm), *M. truncatula* (Mt), *P. trichocarpa* (Pt), and *P. patens* (Pp). Similar residues are highlighted in gray and identical residues in black.

imaging 2 microscope under DIC optics. Images were taken with an Axiocam HRC CCD camera (Zeiss) using the Axiovision 3.1 program.

Aniline Blue Staining of Pollen Tubes

Flowers were emasculated and pollinated 48 h later. After 2 more days, the pistils were harvested, and the replum was cut open under a dissecting scope and fixed for 1.5 h in an acetic acid/ethanol solution (1:9 [v/v]). The pistils were then softened overnight in a 5 M NaOH solution. Pistils were then stained for 10 min in a 0.1% aniline blue, 0.1 M K_2PO_4 buffer, pH 8.3, solution. After this, the pistils were cut open under a dissecting scope and observed with a Zeiss Axioplan imaging 2 microscope fitted with an excitation filter (BP 365/12), a chromatic beam splitter (FT 365), and a barrier filter (LP 397) (*lre-2*, *lre-3*, and *lre-4*) or with a ×40 objective (Nikon) with 340- to 380-nm excitation, 400-nm beamsplitter, and 420 long-pass filter set (Nikon) (*lre-1*).

In Situ Hybridization

Flowers or isolated gynoecia of wild-type plants were fixed in 4% paraformaldehyde and embedded in Paraplast (Fisher Scientific). Sections of 12-μm thickness were cut using a Leica microtome and mounted on ProbeOnPlus slides (Fischer Biotech). A fragment of 181 bp was amplified using sense (5′-GGTTGGAAACAGAATGTGA-3′) and antisense (5′-CTGTGCACAATCACTATTC-3′) primers, and hybridizations were conducted as described (Vielle-Calzada et al., 1999).

GFP-LORELEI Localization

The GFP fusion construct was introduced into *Arabidopsis* mesophyll protoplasts by polyethylene glycol–mediated transfection according to Yoo et al. (2007). Twelve to sixteen hours after transfection, the GFP signal was observed under an Eclipse E600 microscope equipped with

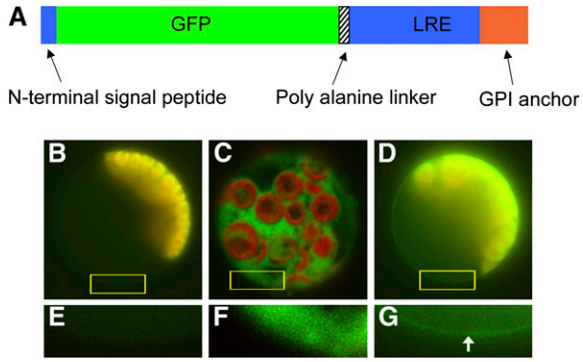

Figure 5. Subcellular Localization of LORELEI.

(A) Schematic representation of the GFP-LRE construct. The GFP is sandwiched between the N-terminal signal peptide and the rest of the LORELEI protein (central domain and GPI anchor domain). The predicted GPI anchor domain is shown in orange. An 8x Ala linker was added at the junction between the GFP and the major part of LORELEI.

(B) to **(G)** Epifluorescence detection of GFP-LRE in transfected protoplasts. The GFP fusion protein (green) appeared at the cell periphery as a line in transfected mesophyll protoplasts in which chloroplast autofluorescence (red) was also detected (**[D]**; detail from boxed region is shown in **[G]**, with the arrow showing the thin fluorescent band around at the periphery of the cell). In protoplasts transfected with GFP only, the GFP protein (green) was seen throughout the cell, with no preference for the cell periphery. The autofluorescence from the chloroplasts appears in red (**[C]**; detail from boxed region is shown in **[F]**). In untransfected protoplasts, only chloroplast autofluorescence was detected (red) (**[B]**; detail from boxed region is shown in **[E]**). Exposure times for the pictures were as follows: 1 s for the green and red channels of the untransfected control (**[B]** and **[E]**), 0.6 s for the green and red channels of GFP (**[C]** and **[F]**), and 0.8 s for the green channel and 1 s for the red channel of GFP-LRE (**[D]** and **[G]**).

epifluorescence optics (Nikon) and captured with an Orca CCD camera (Hamamatsu Photonics) using the MetaMorph software package (Molecular Devices). Filter sets for GFP (green) and Texas Red (red) (Semrock) were used. Images were then assembled with the Adobe Photoshop software package.

Arabidopsis Genomic DNA Extraction

One hundred milligrams of tissue was collected and ground in liquid nitrogen. Five hundred microliters of CTAB extraction buffer (2% CTAB, 1.4 M NaCl, 0.2 M EDTA, and 0.1 M Tris-HCl) was added, followed by 30 min of incubation at 65°C. Five hundred microliters of chloroform was added, and the sample was vortexed and spun at 12,000*g* for 10 min. The aqueous phase was collected and the DNA precipitated by adding 350 μL of isopropanol, followed by spinning at 12,000*g* for 20 min. The DNA was washed with 500 μL of ethanol 70% and dried. The pellet was resuspended in TE buffer (10 mM Tris-HCl and 1 mM EDTA).

T-DNA Lines

The T-DNA lines SALK_040289, SALK_007165, SALK_059671, and SALK_135772 were described by Alonso et al. (2003). The line SAIL_8_C08 was described by Sessions et al. (2002). The lines SALK_040289 and SAIL_8_C08 are *lre-3* and *lre-4*, respectively.

Molecular Analysis of the *une17* Line and T-DNA Lines

The 5′ flanking sequence isolation of *une17* was described by Pagnussat et al. (2005). The 3′ flanking sequence of the *Ds* element was isolated using TAIL-PCR (Liu et al., 1995). The positions of both the 5′ and 3′ ends of the *Ds* element were checked using a gene-specific primer and a *Ds*-specific primer (5′-AGACGATGCGGAACAATCCATGTTG-3′ and 5′-TCCGTTCCGTTTTCGTTTTTTAC-3′ for the 5′ flanking sequence and 5′-GGCTGCAACAATGCAGATCCTGGTA-3′ and 5′-CCGGTATATCCCGTTTTCG-3′ for the 3′ flanking sequence). The PCR products were then purified and sequenced.

The SALK lines flanking sequences were checked using the Lba1 primer (5′-TGGTTCACGTAGTGGGCCATCG-3′) with the following gene-specific primers: 5′-CCTGAAAACGTCTCAGGGAGCTA-3′ for SALK_007165, 5′-AATTGTTGCCGGAGCCAGAT-3′ for SALK_059671, 5′-TCATTATTGCACTATCGACCTTAGGC-3′ for SALK_135772, and 5′-TGGTTGGAAACAGAATGTGAAGTGA-3′ for SALK_040289. For the line SAIL_8_C08, the following primers were used to amplify the left border flanking sequence: 5′-TTCATAACCAATCTCGATACAC-3′ and 5′-TGCTGCAACCGCTGTTTTTG-3′. The right border sequence of SALK_040289 was amplified using 5′-AACGGCTTGTCCCGCGTCAT-3′ and 5′-TGGCTCTTTCAATTTCCTTTGATTG-3′.

Both the left border and right border flanking sequences of SALK_040289 were purified and sequenced.

Plasmids

The plasmid JatY53G03 was obtained from the JatY collection of the John Innes Centre (http://jicgenomelab.co.uk/libraries.html). The pC450 was constructed from a pCAMBIA 1300 vector (Cambia). The annotated *At4g26450* gene was amplified with the following primers 5′-ATATATGTCGACTGGGCTCAAGCTGAAACGTG-3′ and 5′-ATATATGTCGACCCGTGTGCTCTGTCTGCATT-3′, producing a 10-kb fragment. The pCAMBIA 1300 and the PCR fragment were digested with *Sal*I and ligated together to form pC450.

A 2.6-kb fragment containing the sequence of *LORELEI* along with 1.4 kb of promoter and 0.45 kb of terminator sequences was amplified with the following primers 5′-ATATATGTCGACAATTGTTGCCGGAGCCAGAT-3′ and 5′-ATATATGTCGACCCGTGTGCTCTGTCTGCATT-3′. This fragment was cloned in pCAMBIA 1300 with *Sal*I to create pCLRE.

To generate the GFP-LORELEI fusion, the LORELEI sequence, minus the first 69 bp corresponding to the N-terminal signal peptide was amplified by PCR. A *Hin*dIII and an 8x Ala linker was added to the 5′ with the primer, and an *Eco*RI site was added after the STOP codon at the 3′ with the primers. The primers used are 5′-ATATATAAGCTTGCGGCTGCCGCGGCAGCGGCAGCCTCGGATGGTGTGTTTGAAT-3′ and 5′-ATATATGAATTCTCAAGTCAACACTAACAAAG-3′. EGFP was modified through PCR. The sequence corresponding to the N-terminal signal peptide was added in three successive rounds of PCR as well as an Asp-718 restriction site at the 5′ end. A *Hin*dIII site was added at the 3′ end. The primers used for the 5′ end elongation were 5′-ATATATTCTCTCTCCTCTTCAAGTTCCATAATGAGTAAAGGAGAAGAACT-3′, 5′-ATATATCTTCTTTCTGATGGCACTGTTGGTATCTCTCTCCTCTTCAAGTTC-3′, and 5′-ATATATGGTACCATGGAGCTGATATTATTATTCTTCTTTCTGATGGCACTGT-3′, successively. The 3′ primer was 5′- ATATATAAGCTTTTTGTATAGTTCATCCATGC-3′. The EGFP fragment and the LORELEI fragment were combined in a vector containing a 35S promoter and a NOS terminator described by Griffith et al. (2007). The resulting plasmid was named p35s:GFP-LRE.

Accession Numbers

Sequence data from this article can be found in the Arabidopsis Genome Initiative or GenBank/EMBL databases under the following accession

numbers: *Lorelei*, EU727071; At5g265170, BT001157; At2g20700, BT012124; At4g28280, BT011635; Mt LORELEI-related 1, CU207236; Mt LORELEI-related 2, AC174340; Mt LORELEI-related 3, AC174340; Os 02g0721700, NM_001054497; Os 09g02978, NM_001069341; Pt LORELEI-related1, POP055-H02; Vr Arg8, AB013853; Zm 20282, DQ245780; Zm DQ244578, DQ244578; and Pp 171056, XM_001780105.

Supplemental Data

The following materials are available in the online version of this article.

Supplemental Figure 1. RT-PCR on *lre-3* Homozygous and Heterozygous Plants.

Supplemental Table 1. Real-Time PCR for *LORELEI*.

Supplemental Methods. RT-PCR Using *Arabidopsis* Total RNA, Real-Time PCR, and RT-PCR on *lre-3*/+ and *lre-3*/*lre-3* Plants.

Supplemental Results. Identification of a New ORF in the *At4g26450* Locus, *LORELEI* Expression in *Arabidopsis* Organs, and *lre-3* as a Null Mutation.

ACKNOWLEDGMENTS

We thank Ueli Grossniklaus for generously providing cell-specific marker lines used in this study, Quy Ngo for many helpful suggestions, and Thomas Berleth for discussions. This work was supported by National Science Foundation Grants 2010 0313501 and IOS-0745167 to V.S. and USDA/CSREES/NRICGP Grant 2005-35304-16031 to B.L. Research in the J.-P.V.-C. lab is supported by CONCyTEG, UC-MEXUS, and HHMI. A.C. was supported by an EMBO Long-Term Fellowship.

Received June 27, 2008; revised October 1, 2008; accepted November 4, 2008; published November 21, 2008.

REFERENCES

Acosta-Garcia, G., and Vielle-Calzada, J.P. (2004). A classical arabinogalactan protein is essential for the initiation of female gametogenesis in Arabidopsis. Plant Cell **16:** 2614–2628.

Alfieri, J.A., Martin, A.D., Takeda, J., Kondoh, G., Myles, D.G., and Primakoff, P. (2003). Infertility in female mice with an oocyte specific knockout of GPI-anchored proteins. J. Cell Sci. **111:** 2149–2155.

Alonso, J.M., et al. (2003). Genome-wide insertional mutagenesis of *Arabidopsis thaliana*. Science **301:** 653–657.

Altschul, S.F., Gish, W., Miller, W., Myers, E.W., and Lipman, D.J. (1990). Basic local alignment search tool. J. Mol. Biol. **215:** 403–410.

Bechtold, N., and Pelletier, G. (1998). *In planta Agrobacterium*-mediated transformation of adult *Arabidopsis thaliana* plants by vacuum infiltration. Methods Mol. Biol. **82:** 259–266.

Bendtsen, J.D., Nielsen, H., von Heijne, G., and Brunak, S. (2004). Improved prediction of signal peptides: SignalP 3.0. J. Mol. Biol. **340:** 783–795.

Boisson-Dernier, A., Frietsch, S., Kim, T.H., Dizon, M.B., and Schroeder, J.I. (2008). The peroxin loss-of-function mutation *abstinence by mutual consent* disrupts male-female gametophyte recognition. Curr. Biol. **18:** 63–68.

Chen, Y.H., Li, H.J., Shi, D.Q., Yuan, L., Liu, J., Sreenivasan, R., Baskar, R., Grossniklaus, U., and Yang, W.C. (2007). The central cell plays a critical role in pollen tube guidance in *Arabidopsis.* Plant Cell **19:** 3563–3577.

Coppinger, P., Repetti, P.P., Day, B., Dahlbeck, D., Mehlert, A., and Staskawicz, B.J. (2004). Overexpression of the plasma membrane-localized NDR1 protein results in enhanced bacterial disease resistance in *Arabidopsis thaliana.* Plant J. **40:** 225–237.

Day, B., Dahlbeck, D., and Staskawicz, B.J. (2006). NDR1 interaction with RIN4 mediates the differential activation of multiple disease resistance pathways in *Arabidopsis.* Plant Cell **18:** 2782–2791.

Dresselhaus, T. (2006). Cell-cell communication during double fertilization. Curr. Opin. Plant Biol. **9:** 41–47.

Eisenhaber, B., Wildpaner, M., Schultz, C.J., Borner, G.H., Dupree, P., and Eisenhaber, F. (2003). Glycosylphosphatidylinositol lipid anchoring of plant proteins. Sensitive prediction from sequence- and genome-wide studies for Arabidopsis and rice. Plant Physiol. **133:** 1691–1701.

Emanuelsson, O., Nielsen, H., Brunak, S., and von Heijne, G. (2000). Predicting subcellular localization of proteins based on their N-terminal amino acid sequence. J. Mol. Biol. **300:** 1005–1016.

Escobar-Restrepo, J.M., Huck, N., Kessler, S., Gagliardini, V., Gheyselinck, J., Yang, W.C., and Grossniklaus, U. (2007). The FERONIA receptor-like kinase mediates male-female interactions during pollen tube reception. Science **317:** 656–660.

Gillmor, C.S., Lukowitz, W., Brinistool, G., Sedbrook, J.C., Hamann, T., Pointdexter, P., and Somerville, C. (2005). Glycosylphosphatidylinositol-anchored proteins are required for cell wall synthesis and morphogenesis in Arabidopsis. Plant Cell **17:** 1128–1140.

Griffith, M.E., Mayer, U., Capron, A., Ngo, Q.A., Surendrarao, A., McClinton, R., Jürgens, G., and Sundaresan, V. (2007). The *TORMOZ* gene encodes a nucleolar protein required for regulated division planes and embryo development in *Arabidopsis.* Plant Cell **19:** 2246–2263.

Gross-Hardt, R., Kägi, C., Baumann, N., Moore, J.M., Baskar, R., Gagliano, W.B., Jürgens, G., and Grossniklaus, U. (2007). *LACHESIS* restricts gametic cell fate in the female gametophyte of *Arabidopsis.* PLoS Biol. **5:** e47.

Guitton, A.E., Page, D.R., Chambrier, P., Lionnet, C., Faure, J.E., Grossniklaus, U., and Berger, F. (2004). Identification of new members of Fertilisation Independent Seed Polycomb Group pathway involved in the control of seed development in *Arabidopsis thaliana.* Development **131:** 2971–2981.

Higashiyama, T., Yabe, S., Sasaki, N., Nishimura, Y., Miyagishima, S., Kuroiwa, H., and Kuroiwa, T. (2001). Pollen tube attraction by the synergid cell. Science **293:** 1480–1483.

Huck, N., Moore, J.M., Federer, M., and Grossniklaus, U. (2003). The *Arabidopsis* mutant *feronia* disrupts the female gametophytic control of pollen tube reception. Development **130:** 2149–2159.

Kondoh, G., Tojo, H., Nakatani, Y., Komazawa, N., Murata, C., Yamagata, K., Maeda, Y., Kinoshita, T., Okabe, M., Taguchi, R., and Takeda, J. (2005). Angiotensin-converting enzyme is a GPI-anchored protein releasing factor crucial for fertilization. Nat. Med. **11:** 160–166.

Lalanne, E., Honys, D., Johnson, A., Borner, G.H.H., Lilley, K.S., Dupree, P., Grossniklaus, U., and Twell, D. (2004). *SETH1* and *SETH2*, two components of the glycosylphophatidylinositol anchor biosynthetic pathway, are required for pollen germination and tube growth in Arabidopsis. Plant Cell **16:** 229–240.

Larkin, M.A., et al. (2007). Clustal W and Clustal X version 2.0. Bioinformatics **23:** 2947–2948.

Liu, C.M., and Meinke, D.W. (1998). The titan mutants of Arabidopsis are disrupted in mitosis and cell cycle control during seed development. Plant J. **16:** 21–31.

Liu, Y.G., Chen, Y., and Zhang, Q. (1995). Amplification of genomic sequences flanking T-DNA insertions by thermal asymmetric interlaced polymerase chain reaction. Methods Mol. Biol. **286:** 341–348.

Liu, Y.G., Mitsukawa, N., Oosumi, T., and Whittier, R.F. (2005). Efficient isolation and mapping of *Arabidopsis thaliana* T-DNA insert junctions by thermal asymmetric interlaced PCR. Plant J. **8:** 457–463.

Mayor, S. (2005). ACEing GPI release. Nat. Struct. Mol. Biol. **12:** 107–108.

Muñiz, M., and Riezman, H. (2002). Intracellular transport of GPI-anchored proteins. EMBO J. **19:** 10–15.

Nadeau, J.A. and Sack, F.D. (2002). Control of stomatal distribution on the *Arabidopsis* leaf surface. Science **296:** 1697–1700.

Nielsen, H., Engelbrecht, J., Brunak, S., and von Heijne, G. (1997). Identification of prokaryotic and eukaryotic signal peptides and prediction of their cleavage sites. Protein Eng. **10:** 1–6.

Orlean, P., and Menon, A.K. (2007). Thematic review series: Lipid posttranslational modifications. GPI anchoring of protein in yeast and mammalian cells, or: how we learned to stop worrying and love glycophospholipids. J. Lipid Res. **48:** 993–1011.

Pagnussat, G.C., Yu, H.J., Ngo, Q.A., Rajani, S., Mayalagu, S., Johnson, C.S., Capron, A., Xie, L.F., Ye, D., and Sundaresan, V. (2005). Genetic and molecular identification of genes required for female gametophyte development and function in *Arabidopsis*. Development **132:** 603–614.

Primakoff, P., and Myles, D.G. (2007). Cell-cell membrane fusion during mammalian fertilization. FEBS Lett. **581:** 2174–2180.

Rotman, N., Rozier, F., Boavida, L., Dumas, C., Berger, F., and Faure, J.E. (2003). Female control of male gamete delivery during fertilization in *Arabidopsis thaliana.* Curr. Biol. **13:** 432–436.

Schindelman, G., Morikami, A., Jung, J., Baskin, T.I., Carpita, N.C., Derbyshire, P., McCann, M.C., and Benfey, P.N. (2001). COBRA encodes a putative GPI-anchored protein, which is polarly localized and necessary for oriented cell expansion in *Arabidopsis.* Genes Dev. **15:** 1115–1127.

Sessions, A., et al. (2002). A high-throughput Arabidopsis reverse genetics system. Plant Cell **14:** 2985–2994.

Sharom, F.J., and Lehto, M.T. (2002). Glycosylphosphatidylinositol-anchored proteins: Structure, function, and cleavage by phosphatidylinositol-specific phospholipase C. Biochem. Cell. Biol. **80:** 535–549.

Tzafrir, I., Pena-Muralla, R., Dickerman, A., Berg, M., Rogers, R., Hutchens, S., Sweeney, T.C., McElver, J., Aux, G., Patton, D., and Meinke, D. (2004). Identification of genes required for embryo development in Arabidopsis. Plant Physiol. **135:** 1206–1220.

van Meer, G. (2002). Cell biology. The different hues of lipid rafts. Science **296:** 855–857.

Vieira, A., and Miller, D.J. (2006). Gamete interaction: is it species-specific? Mol. Reprod. Dev. **73:** 1422–1429.

Vielle-Calzada, J.P., Thomas, J., Spillane, C., Coluccio, A., Hoeppner, M., and Grossniklaus, U. (1999). Maintenance of genomic imprinting in the *Arabidopsis medea* locus requires zygotic *DDM1* activity. Genes Dev. **13:** 2971–2982.

Wassarman, P.M. (1999). Mammalian fertilization: molecular aspects of gamete adhesion, exocytosis, and fusion. Cell **96:** 175–183.

Xu, X.M., and Møller, S.G. (2006). AtSufE is an essential activator of plastidic and mitochondrial desulfurases in *Arabidopsis.* EMBO J. **25:** 900–909.

Yoo, S.D., Cho, Y.H., and Sheen, J. (2007). *Arabidopsis* mesophyll protoplasts: a versatile cell system for transient gene expression analysis. Nat. Protocols **2:** 1565–1572.

Zheng, H., Kunst, L., Hawes, C., and Moore, I. (2003). A GFP-based assay reveals a role for RHD3 in transport between the endoplasmic reticulum and Golgi apparatus. Plant J. **37:** 398–414.

Maternal Control of Male-Gamete Delivery in *Arabidopsis* Involves a Putative GPI-Anchored Protein Encoded by the *LORELEI* Gene

Arnaud Capron, Mathieu Gourgues, Lissiene S. Neiva, Jean-Emmanuel Faure, Frederic Berger, Gabriela Pagnussat, Anjali Krishnan, Cesar Alvarez-Mejia, Jean-Philippe Vielle-Calzada, Yuh-Ru Lee, Bo Liu and Venkatesan Sundaresan

Plant Cell 2008;20;3038-3049; originally published online November 21, 2008;
DOI 10.1105/tpc.108.061713